Supporting Information for

A dithiacyclam-coordinated silver(I) polymer with anti-cancer stem cell activity

Alice Johnson,[*a] Linda Iffland,[b] Kuldip Singh,[a] Ulf-Peter Apfel,[*b,c] and Kogularamanan Suntharalingam[*a]

[a] School of Chemistry, University of Leicester, Leicester, UK
[b] Ruhr-Universität Bochum, Anorganische Chemie I, Universitätsstraße 150, 44801 Bochum, Germany
[c] Fraunhofer UMSICHT, Osterfelder Str. 3, 46047 Oberhausen, Germany

* To whom correspondence should be addressed:
Email: k.suntharalingam@leicester.ac.uk; ulf.apfel@rub.de; alice.johnson@leicester.ac.uk

Table of Content

Fig. S11 ESI (positive mode) mass spectrum for compound **1** after 0 h in H_2O:DMSO (100:1) at 37 °C.

Fig. S12 ESI (positive mode) mass spectrum for compound **1** after 24 h in H_2O:DMSO (100:1) at 37 °C.

Fig. S13 ESI (positive mode) mass spectrum for compound **1** after 48 h in H_2O:DMSO (100:1) at 37 °C.

Fig. S14 ESI (positive mode) mass spectrum for compound **1** after 72 h in H_2O:DMSO (100:1) at 37 °C.

Fig. S15 Cell viability (% of control) vs concentration (μM) for complex **1** in HMLER cells.

Fig. S16 Cell viability (% of control) vs concentration (μM) for complex **1** in HMLER-shEcad cells.

Fig. S17 Cell viability (% of control) vs concentration (μM) for $\mathbf{L^1}$ in HMLER cells.

Fig. S18 Cell viability (% of control) vs concentration (μM) for $\mathbf{L^1}$ in HMLER-shEcad cells.

Fig. S19 Cell viability (% of control) vs concentration (μM) for $AgPF_6$ in HMLER cells.

Fig. S20 Cell viability (% of control) vs concentration (μM) for $AgPF_6$ in HMLER-shEcad cells.

Fig. S21 Cell viability (% of control) vs concentration (μM) for a 1:1 mixture of $\mathbf{L^1}$ and $AgPF_6$ in HMLER-shEcad cells.

Fig. S22 Cell viability (% of control) vs concentration (μM) for complex **1** in BEAS-2B cells.

Fig. S23 Cell viability (% of control) vs concentration (μM) for complex **1** in MCF10A cells.

Fig. S24 Cell viability (% of control) vs concentration (μM) for complex **1** in HEK 293 cells.

Fig. S25 Mammosphere viability (% of control) vs concentration (μM) for complex **1** in HMLER-shEcad mammospheres.

Fig. S26 Mammosphere viability (% of control) vs concentration (μM) for $\mathbf{L^1}$ in HMLER-shEcad mammospheres.

Fig. S27 ^{1}H NMR spectra (400 MHz) for complex **1** (10 mM) in D_2O:DMSO-d_6 (1:1), in the absence and presence of cysteine (Cys, 10 mM) over the course of 24 h at 37 °C.

Fig. S28 ^{1}H NMR spectra (400 MHz) for complex **1** (10 mM) in DMSO-d_6, in the absence and presence of *N*-acetylcysteine (NAC, 10 mM) over the course of 24 h at 37 °C.

Fig. S29 ^{1}H NMR spectra (400 MHz) for complex **1** (10 mM) in DMSO-d_6, in the absence and presence of glutathione (GSH, 10 mM) over the course of 24 h at 37 °C.

Fig. S30 Chemical structure of the mono-protonated analogue of $\mathbf{L^1}$, $\mathbf{L^1\text{-}H^+}$.

Fig. S31 ^{1}H NMR spectra (400 MHz) for $\mathbf{L^1}$ (10 mM) in D_2O:DMSO-d_6 (1:1), in the absence and presence of HCl (10 mM) after 30 min incubation at 37 °C. The latter represents the ^{1}H NMR spectrum (400 MHz) for the mono-protonated analogue of $\mathbf{L^1}$, $\mathbf{L^1\text{-}H^+}$ in D_2O:DMSO-d_6 (1:1).

Fig. S32 ^{1}H NMR spectra (400 MHz) for $\mathbf{L^1}$ (10 mM) in DMSO-d_6, in the absence and presence of HCl (10 mM) after 30 min incubation at 37 °C. The latter represents the ^{1}H NMR spectrum (400 MHz) for the mono-protonated analogue of $\mathbf{L^1}$, $\mathbf{L^1\text{-}H^+}$ in DMSO-d_6.

Experimental Details

Instrumentation. Mass spectra were recorded on a Micromass Quattro with the electrospray (ESI) technique and on a Kratos Concept 1H (ESI-TOF). ^{1}H, $^{13}C\{^{1}H\}$, $^{31}P\{^{1}H\}$ and $^{19}F\{^{1}H\}$ NMR were recorded at room temperature on a Bruker Avance 400 spectrometer (^{1}H 400.0 MHz, ^{13}C 100.6 MHz, ^{31}P 162.0 MHz, ^{19}F 376.5 MHz) with chemical shifts (δ, ppm) reported relative to the solvent peaks of the deuterated solvent. All *J* values are given in Hz. ICP-MS were measured using a Thermo Scientific ICAP-Qc quadrupole ICP mass spectrometer. Elemental Analysis was performed commercially at London Metropolitan University.

Starting Materials. 1,8-dithia-4-11-diazacyclotetradecane (**L^{1}**) was prepared according to a previously reported procedure.[1] Silver(I) hexafluorophosphate, *N*-acetylcysteine, glutathione, and L-cysteine were purchased from Sigma-Aldrich and used without further purification. Solvents were purchased from Fisher and used without further purification.

Synthesis of [Ag(1,8-dithia-4,11-diazacyclotetradecane)]PF_6, 1. To a solution of 1,8-dithia-4,11-diazacyclotetradecane (46.9 mg, 0.2 mmol) in dichloromethane (10 ml) was added $AgPF_6$ (50.6 mg, 0.2 mmol) and the mixture stirred for 2 h in the dark. The yellow solution was filtered through celite, concentrated under reduced pressure and pentane was added to precipitate a pale-yellow solid which was collected by vacuum filtration and vacuum dried (70.6 mg, 72%); ^{1}H NMR (400 MHz, DMSO) δ 3.04 (s, 1H, NH), 2.86 – 2.82 (m, 4H, 2 × CH_2), 2.80 – 2.78 (m, 2H, CH_2), 2.73 – 2.69 (m, 2H, CH_2), 1.80 (s, 2H, CH_2); ^{13}C NMR (101 MHz, DMSO) δ 50.56 (s), 46.09 (s), 33.62 (s), 32.48 (s), 26.92 (s); ^{31}P NMR (162 MHz, DMSO) δ -144.20 (hept, $^{1}J_{PF}$ = 711.2 Hz, PF_6); ^{19}F NMR (376 MHz, DMSO) δ -70.15 (d, $^{1}J_{FP}$ = 711.2 Hz, PF_6); HR-ESI-QTOF-MS *m/z*: [**1**-PF_6]$^{+}$ Calcd for $C_{10}H_{22}AgN_2S_2$: 343.0269; Found 343.0270; Anal. Calcd. for $C_{10}H_{22}AgF_6N_2PS_2$: C 24.65, H 4.55, N 5.75. Found: C 25.05, H 4.73, N 5.74.

X-ray Crystallography. Crystals were mounted in inert oil on glass fibres and transferred to a Bruker Apex 2000 CCD area detector diffractometer. Data was collected using graphite-monochromated Mo-Kα radiation (λ = 0.71073) at 150(2) K. Scan type ϖ. Absorption corrections based on multiple scans were applied using SADABS[2] or spherical harmonics implemented in SCALE3 ABSPACK scaling algorithm.[3] The structures were solved by direct methods and refined on F2 using the program SHELXT-2016.[4] All non-hydrogen atoms were refined anisotropically. The CCDC deposition number 2053375 contains the supplementary crystallographic data. This data can be obtained free of charge via The Cambridge Crystallography Data Centre.

Measurement of water-octanol partition coefficient (LogP). The LogP value for **1** was determined using the shake-flask method and ICP-MS. The 1-octanol used in this experiment was pre-saturated with water. A DMSO solution of **1** (10 μL, 10 mM) was incubated with 1-octanol (495 μL) and H_2O (495 μL) in a 1.5 mL tube. The tube was shaken at room temperature for 24 h. The two phases were separated by centrifugation and the silver content in the water phase was determined by ICP-MS.

Cell culture. The human mammary epithelial cell lines, HMLER and HMLER-shEcad were kindly donated by Prof. R. A. Weinberg (Whitehead Institute, MIT). HMLER and HMLER-shEcad cells were maintained in Mammary Epithelial Cell Growth Medium (MEGM) with supplements and growth factors (BPE, hydrocortisone, hEGF, insulin, and

gentamicin/amphotericin-B). The BEAS-2B bronchial epithelium cell line was acquired from American Type Culture Collection (ATCC, Manassas, VA, USA) and cultured in RPMI 1640 medium with 2 mM L-glutamine supplemented with 1% penicillin and 10% fetal bovine serum. The cells were grown at 310 K in a humidified atmosphere containing 5% CO2.

Antiproliferative studies: MTT assay. Exponentially growing cells were seeded at a density of approximately 5×10^3 cells per well in 96-well flat-bottomed microplates and allowed to attach for 24 h prior to addition of compounds. Various concentrations of the test compounds (0.1-100 μM) were added and incubated for 72 h at 37 °C (total volume 200 μl). Stock solutions of the compounds were prepared as 10 mM DMSO solutions and diluted using cell media. The final concentration of DMSO in each well was ≤1 %. After 72 h, 20 μl of MTT (4 mg ml^{-1} in PBS) was added to each well and the plates incubated for an additional 4 h at 37 °C. The media/MTT mixture was eliminated and DMSO (100 μl per well) was added to dissolve the formazan precipitates. The optical density was measured at 550 nm using a 96-well multiscanner autoreader. Absorbance values were normalised to (DMSO-containing) control wells and plotted as concentration of compound versus % cell viability. IC_{50} values were interpolated from the resulting dose dependent curves. The reported IC_{50} values are the average of three independent experiments (n = 12).

Tumoursphere formation and viability assay. HMLER-shEcad cells (5×10^3) were plated in ultralow-attachment 96-well plates (Corning) and incubated in MEGM supplemented with B27 (Invitrogen), 20 ng mL^{-1} EGF and 4 μg mL^{-1} heparin (Sigma) for 5 days. Studies were also conducted in the presence of **1** and salinomycin (0–133 mm). Mammospheres treated with **1** and salinomycin (at 2 μM, 8 μM, and their respective IC_{20} values, 5 days) were counted and imaged using an inverted microscope. The viability of the mammospheres was determined by addition of a resazurin-based reagent, TOX8 (Sigma). After incubation for 16 h, the fluorescence of the solutions was read at 590 nm (λ_{ex} = 560 nm). Viable mammospheres reduce the amount of the oxidised TOX8 form (blue) and concurrently increase the amount of the fluorescent TOX8 intermediate (red), indicating the degree of mammosphere cytotoxicity caused by the test compound. Fluorescence values were normalised to DMSO-containing controls and plotted as concentration of test compound versus % mammospheres viability. IC_{50} values were interpolated from the resulting dose dependent curves. The reported IC_{50} values are the average of three independent experiments, each consisting of two replicates per concentration level (overall n = 6).

Cellular uptake. To measure the cellular uptake of **1** and $AgPF_6$ about 1 million HMLER-shEcad cells were treated with **1** or $AgPF_6$ (5 μM) at 37 °C for 24 h. After incubation, the media was removed, the cells were washed with PBS (2 mL × 3) and harvested. The number of cells was counted at this stage, using a haemocytometer. This mitigates any cell death induced by **1** and $AgPF_6$ at the administered concentration and experimental cell loss. The cellular pellets were dissolved in 65% HNO_3 (250 mL) overnight. A cellular pellet of HMLER-shEcad cells treated with **1** was also used to determine the silver content in the nuclear, cytoplasmic and membrane fractions. The Thermo Scientific NE-PER Nuclear and Cytoplasmic Extraction Kit was used to extract and separate the nuclear, cytoplasmic and membrane fractions. The fractions were dissolved in 65% HNO_3 (250 ml final volume) overnight. All samples were diluted 17-fold with water and analysed using inductively coupled plasma mass spectrometry (ICP-MS, Thermo Scientific ICAP-Qc quadrupole ICP mass spectrometer). Silver levels are expressed as mass of Ag (ng) per million cells. Results are presented as the mean of four determinations for each data point.

Intracellular ROS Assay. HMLER-shEcad cells (5×10^3) were seeded in each well of a 96-well plate. After incubating the cells overnight, they were treated with **1** (4 μM for 0.5-24 h) and incubated with 6-carboxy-2′,7′-dichlorodihydrofluorescein diacetate (20 μM) for 90 min. The intracellular ROS level was determined by measuring the fluorescence of the solutions in each well at 529 nm (λ_{ex} = 504 nm).

Immunoblotting Analysis. HMLER-shEcad cells (5×10^6) were incubated with **1** (4 μM and 8 μM for 72 h) at 37 ^{o}C. HMLER-shEcad cells were harvested and isolated as pellets. SDS-PAGE loading buffer (64 mM Tris-HCl (pH 6.8)/ 9.6% glycerol/ 2%SDS/ 5% β-mercaptoethanol/ 0.01% Bromophenol Blue) was added to the pellets, and this was incubated at 95 ^{o}C for 10 min. Cell lysates were resolved by 4-20 % sodium dodecylsulphate polyacylamide gel electrophoresis (SDS-PAGE; 200 V for 25 min) followed by electro transfer to polyvinylidene difluoride membrane, PVDF (350 mA for 1 h). Membranes were blocked in 5% (w/v) non-fat milk in PBST (PBS/0.1% Tween 20) and incubated with the appropriate primary antibodies (Cell Signalling Technology). After incubation with horseradish peroxidase-conjugated secondary antibodies (Cell Signalling Technology), immune complexes were detected with the ECL detection reagent (BioRad) and analysed using a chemiluminescence imager (Bio-Rad ChemiDoc Imaging System).

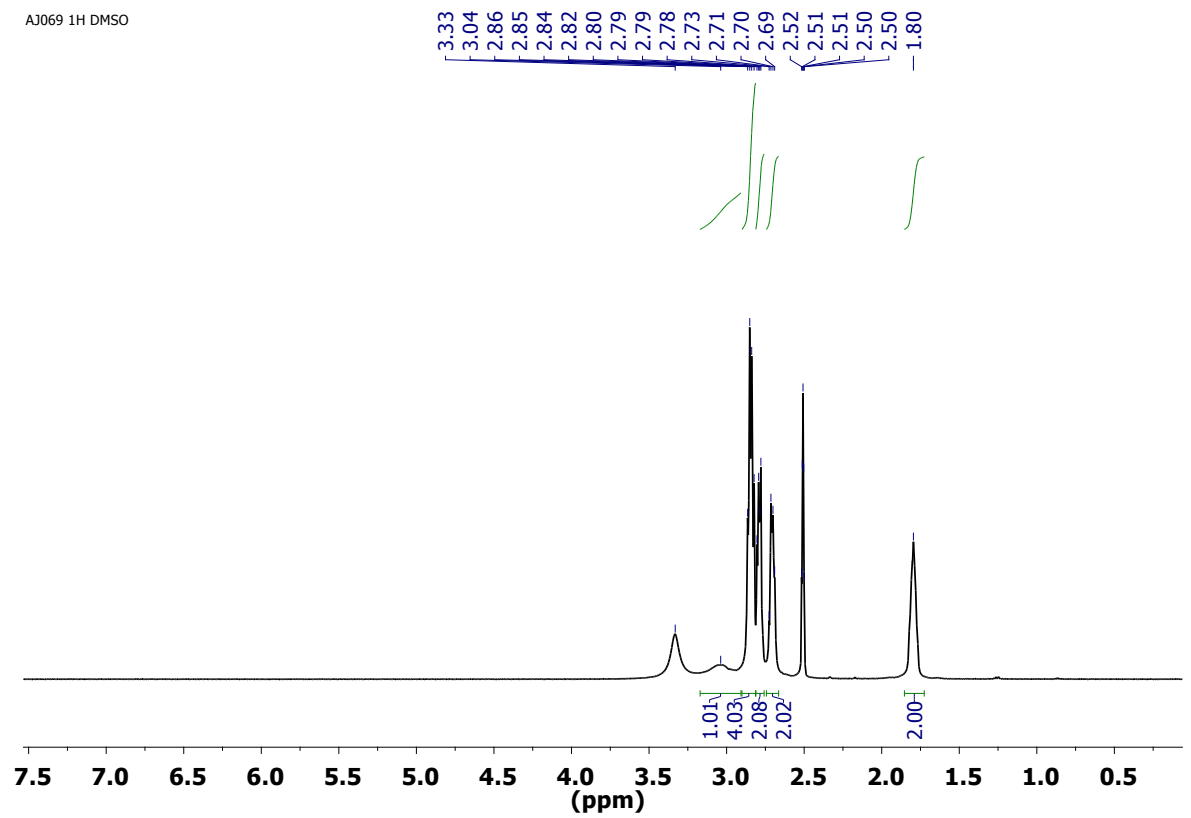

Fig. S1 ^{1}H NMR spectrum (400 MHz, DMSO-d_6) for complex **1**.

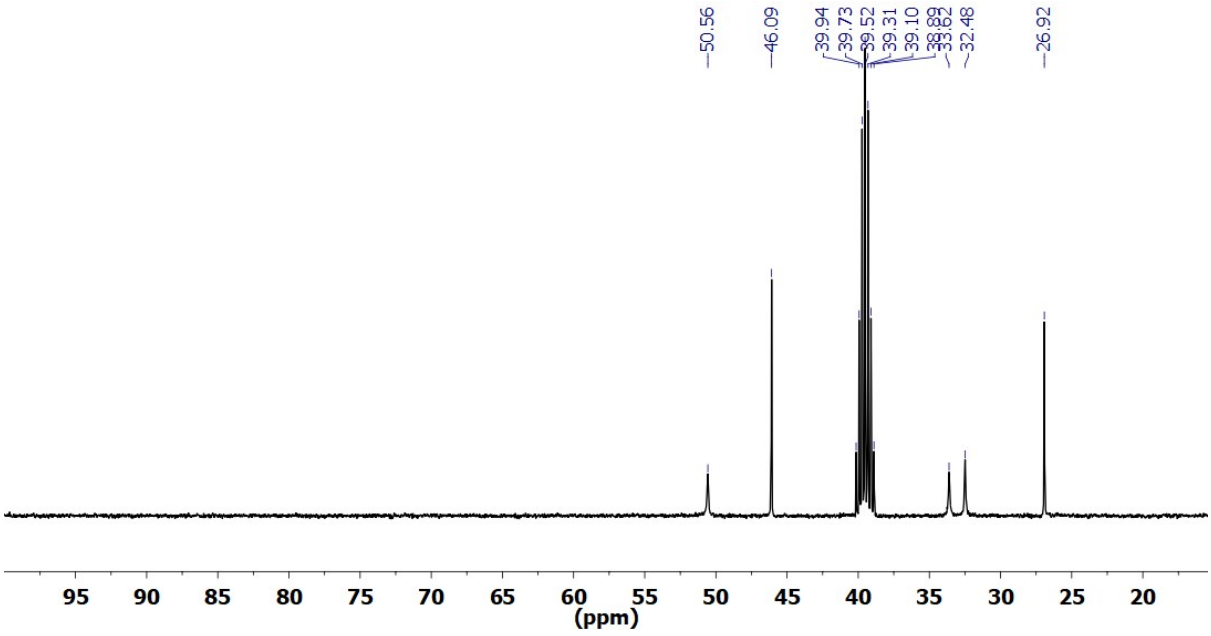

Fig. S2 ^{13}C NMR spectrum (101 MHz, DMSO-d_6) for complex **1**.

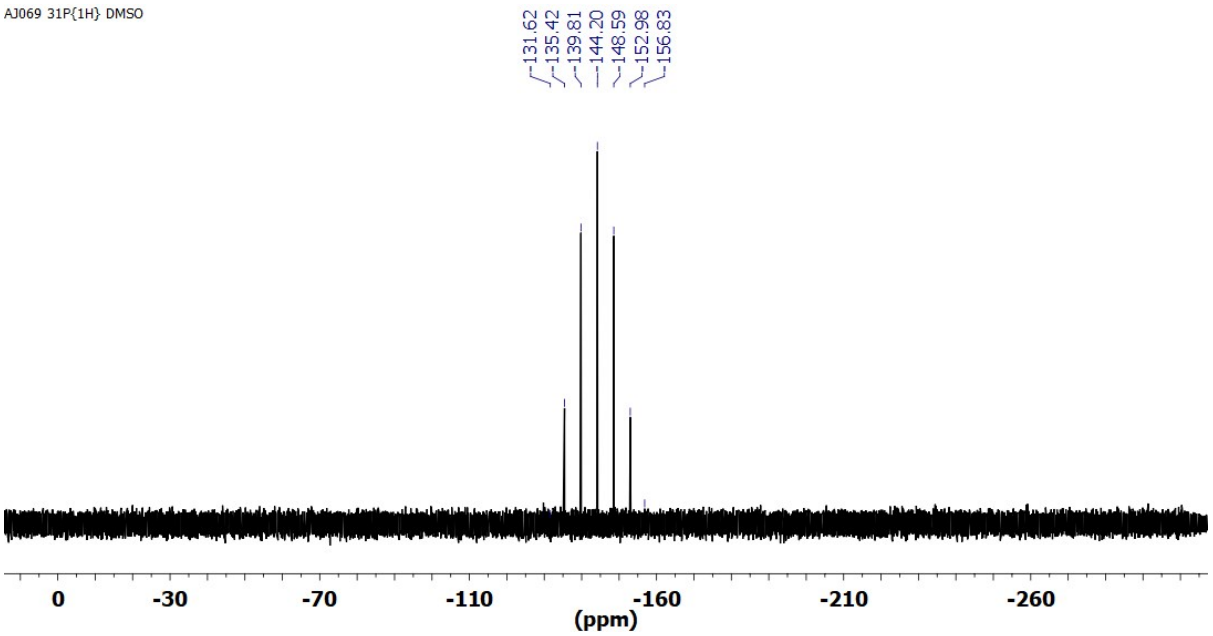

Fig. S3 $^{31}P\{^{1}H\}$ NMR spectrum (162 MHz, DMSO-d_6) for complex **1**.

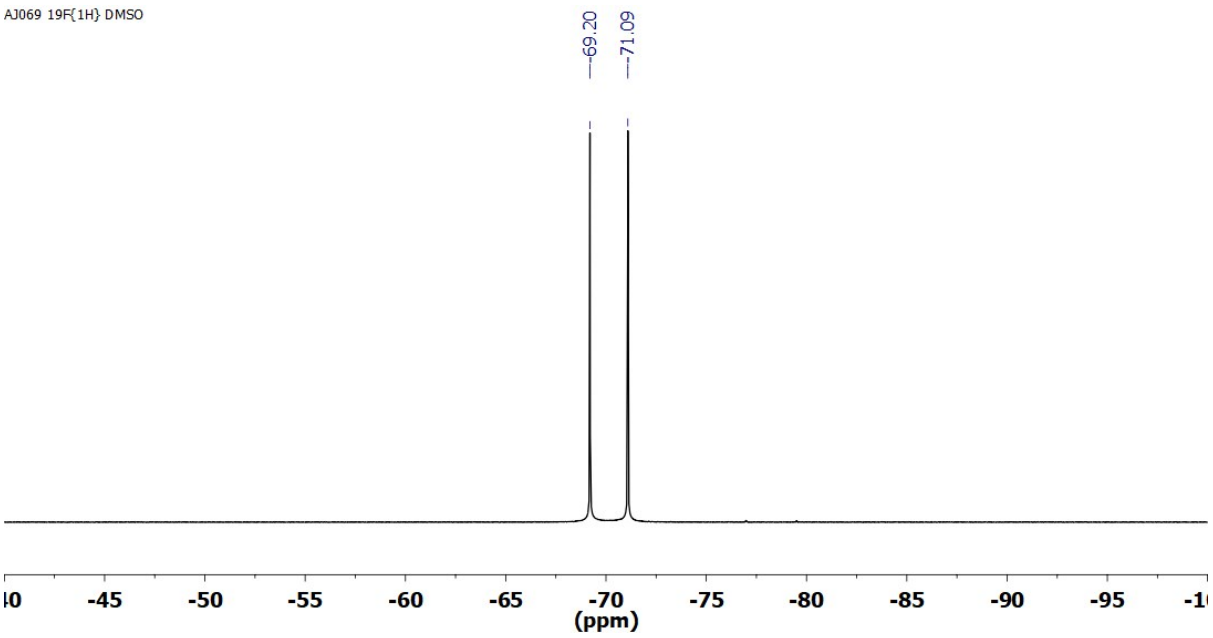

Fig. S4 $^{19}F\{^{1}H\}$ NMR spectrum (376 MHz, DMSO-d_6) for complex **1**.

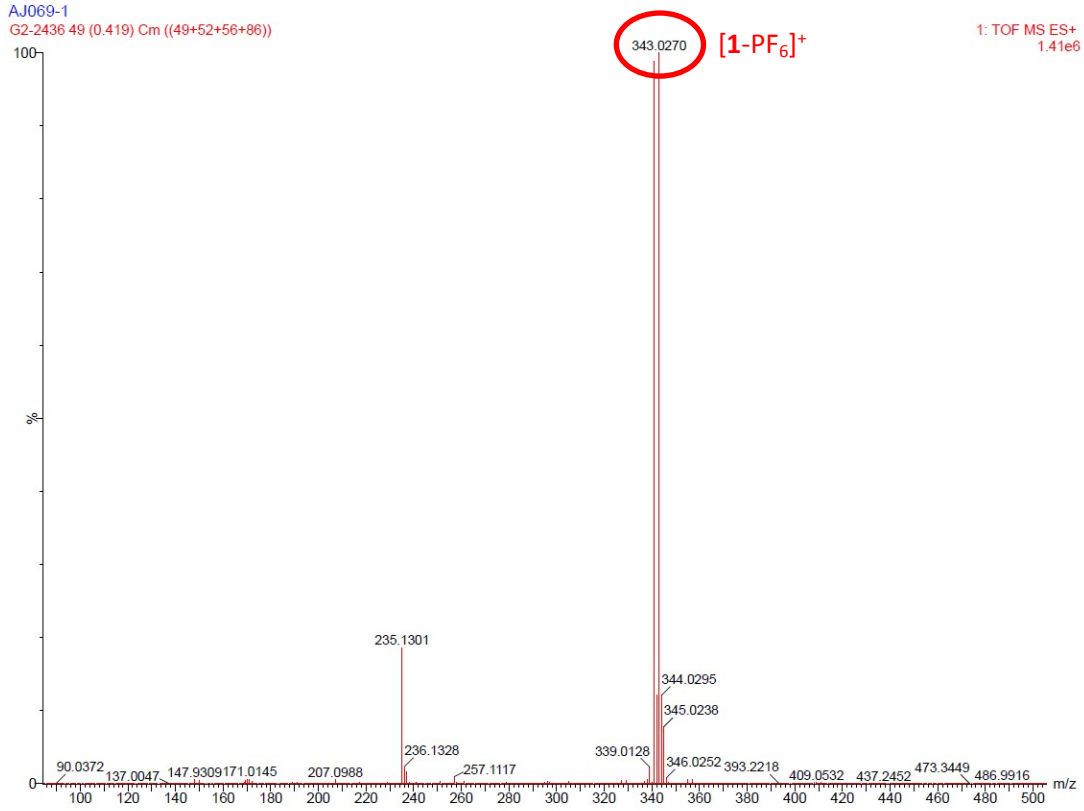

Fig. S5 High-resolution ESI-QTOF mass spectrum for complex **1**.

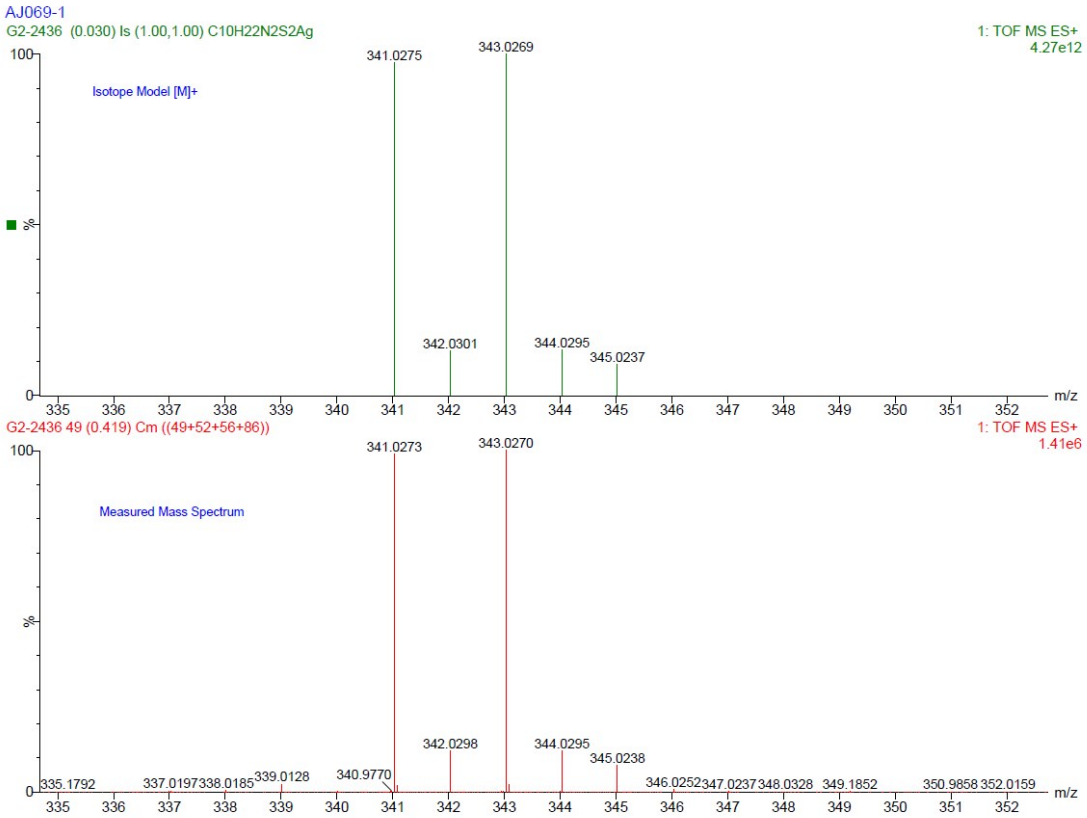

Fig. S6 (Top) Theoretical isotope model for $[\mathbf{1}\text{-}PF_6]^+$ ($C_{10}H_{22}AgN_2S_2$) and (bottom) the experimentally determined high-resolution ESI-QTOF mass spectrum for complex **1**.

Table S1. Selected crystallographic data for complex **1**.

Complex	**1**
Empirical formula	$C_{11}H_{24}AgCl_2F_6N_2PS_2$
Formula weight	572.18
Temperature (K)	150(2)
Wavelength (Å)	0.71073
Crystal system	Monoclinic
Space group	C2/c
Unit cell dimensions	
a (Å)	12.471(6)
b (Å)	16.294(8)
c (Å)	10.405(5)
α (°)	90
β (°)	99.044(10)
γ (°)	90
Volume ($Å^3$)	2088.0(17)
Z	4
Density (calculated) (Mg/m^3)	1.820
Absorption coefficient (mm^{-1})	1.548
θ range (°)	2.07 to 26.00
Reflections collected	8050
R_{int}	0.1163
Completeness (%)	99.9
Data / restraints / parameters	2054 / 0 / 115
Goodness-of-fit on F^2	0.951
R_1 [$I>2\sigma(I)$]	0.0621
wR_2 (all data)	0.1345
Largest diff. peak and hole ($e.Å^{-3}$)	0.743 and -0.758

Table S2. Selected bond lengths (Å) and angles (°) for complex **1**.

Ag(1)-N(1)	2.394(5)	Ag(1)-S(1)	2.5355(19)
N(1A)-Ag(1)-N(1)	108.6(2)	N(1)-Ag(1)-S(1)/ N(1A)-Ag(1)-S(1A)	126.77(13)
S(1A)-Ag(1)-S(1)	136.18(9)	N(1A)-Ag(1)-S(1)/ N(1)-Ag(1)-S(1A)	80.61(13)

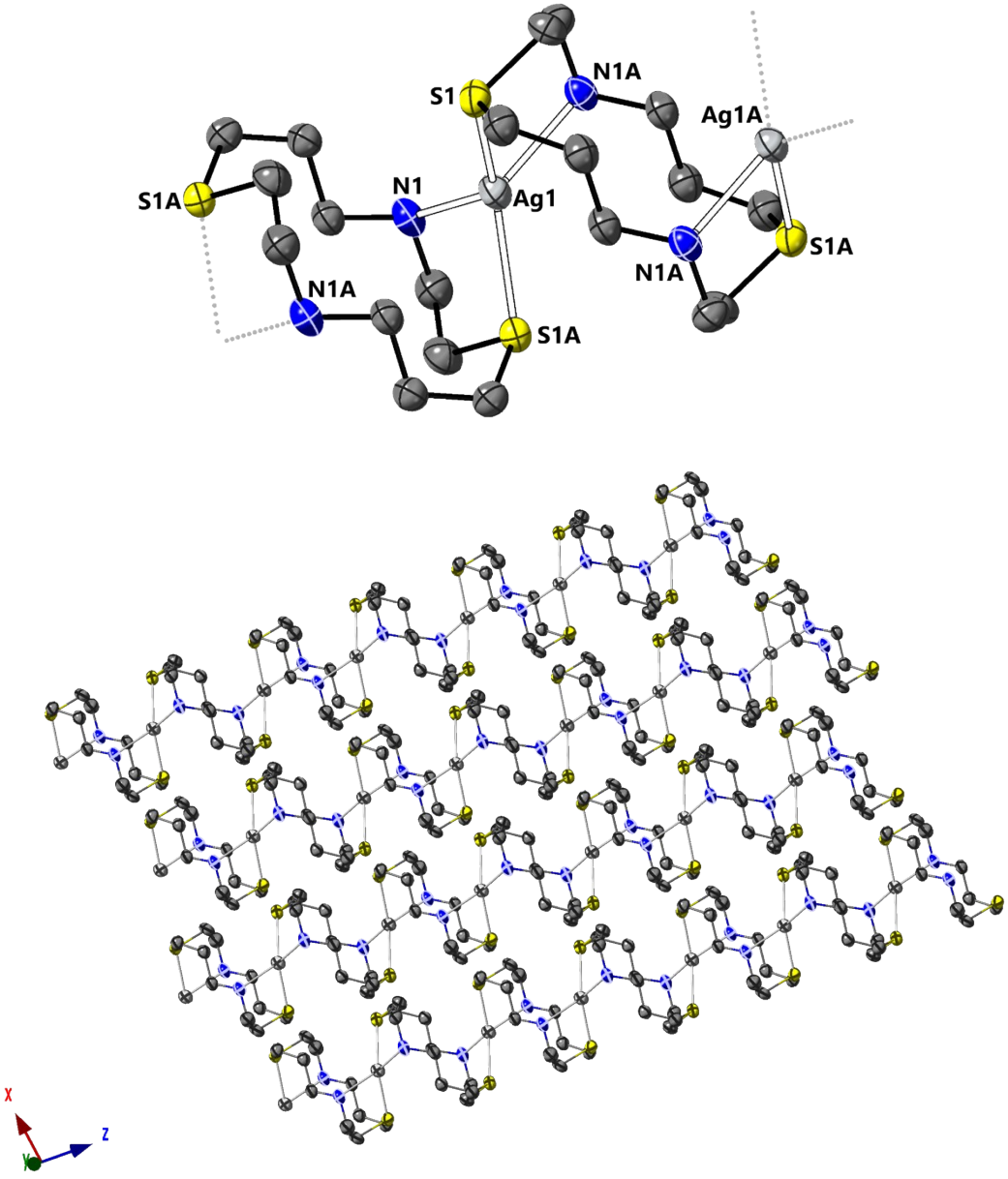

Fig. S7 Structural representation of the crystalline 1D coordination polymer observed for silver(I) complex **1**. Ellipsoids are shown at 50% probability. C in grey, N in dark blue, S in yellow, Ag in silver. H atoms, the co-crystallizing DCM molecule, and the hexafluorophosphate counter anion have been omitted for clarity.

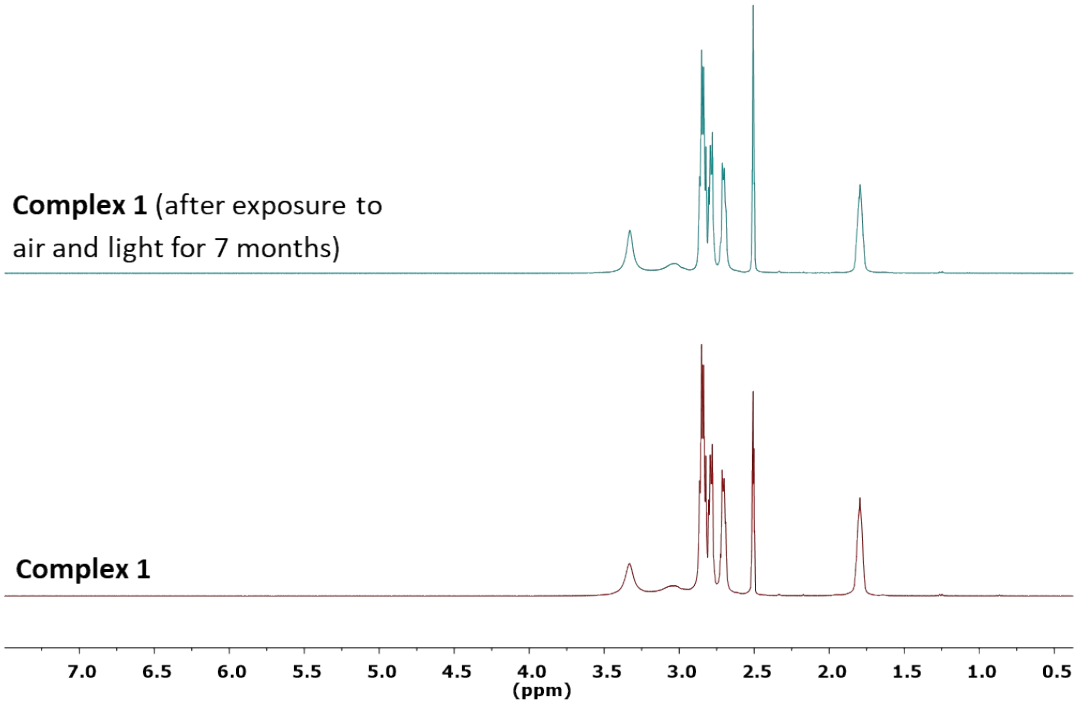

Fig. S8 ^{1}H NMR spectra (400 MHz) for complex **1** in DMSO-d_6 before and after exposure of the solid form to air and light for 7 months.

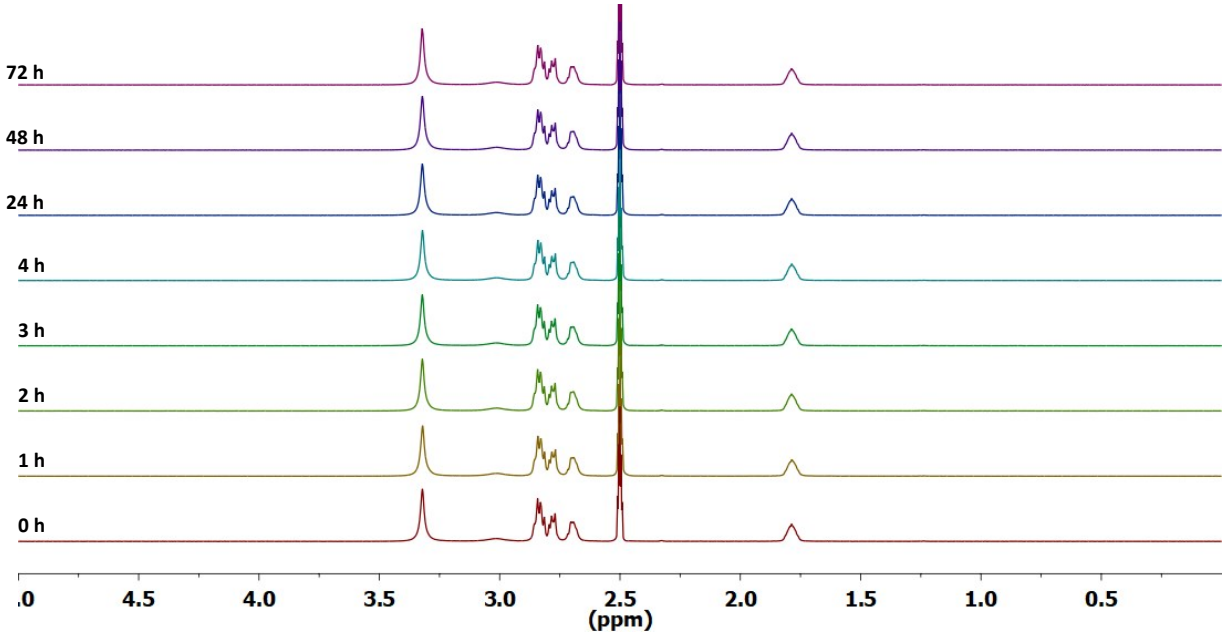

Fig. S9 ^{1}H NMR spectra (400 MHz) for complex **1** in DMSO-d_6 over the course of 72 h at 37 °C.

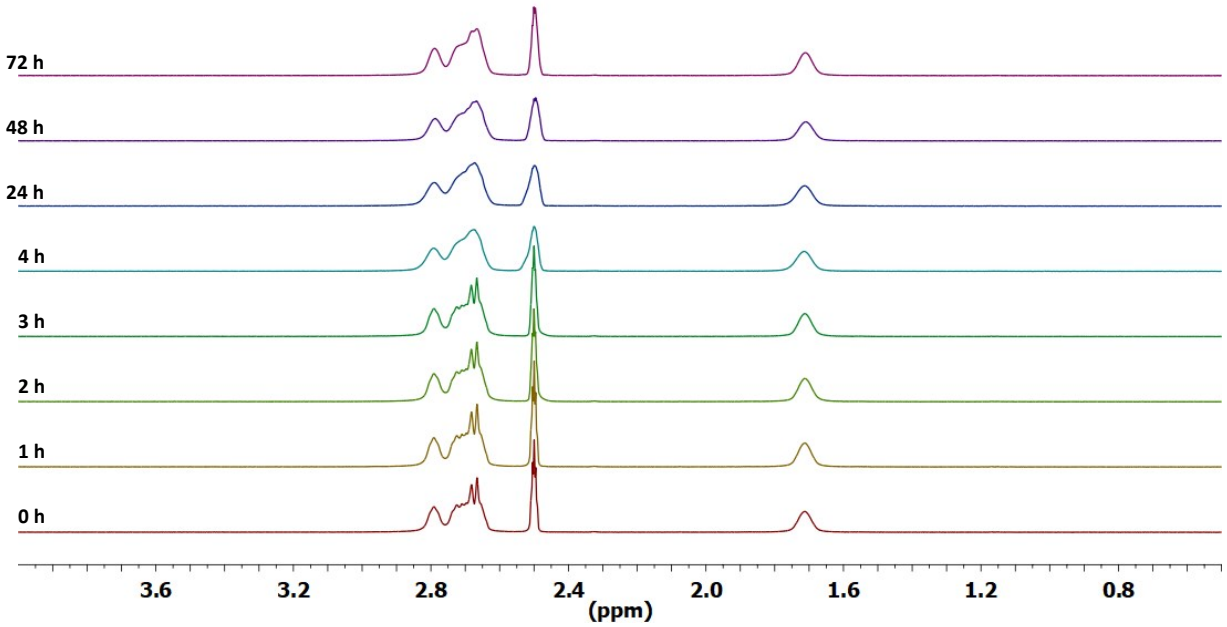

Fig. S10 ^{1}H NMR spectra (400 MHz) for complex **1** in D_2O:DMSO-d_6 (5:1) over the course of 72 h at 37 °C.

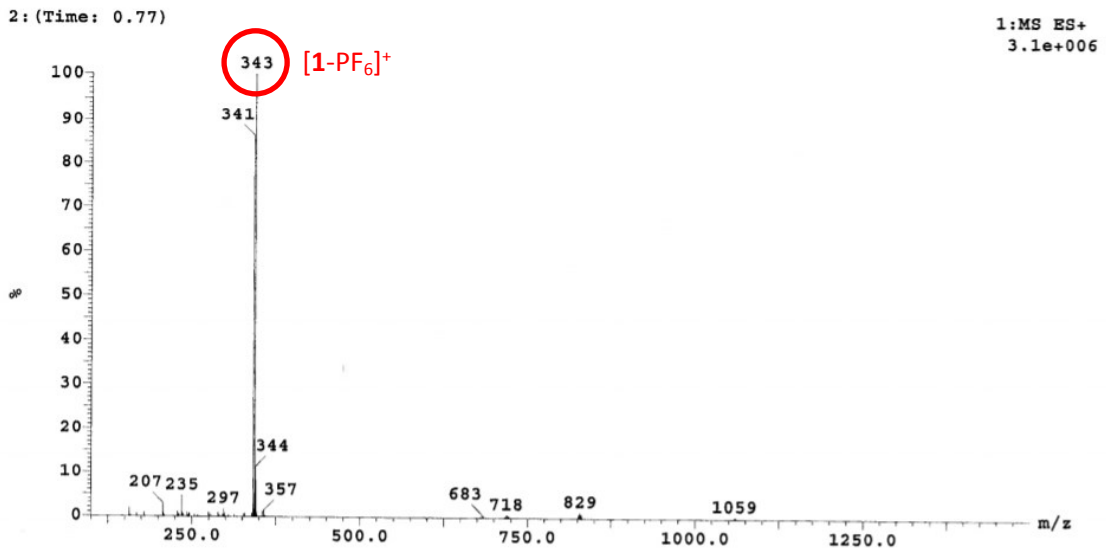

Fig. S11 ESI (positive mode) mass spectrum for compound **1** after 0 h in H_2O:DMSO (100:1) at 37 °C.

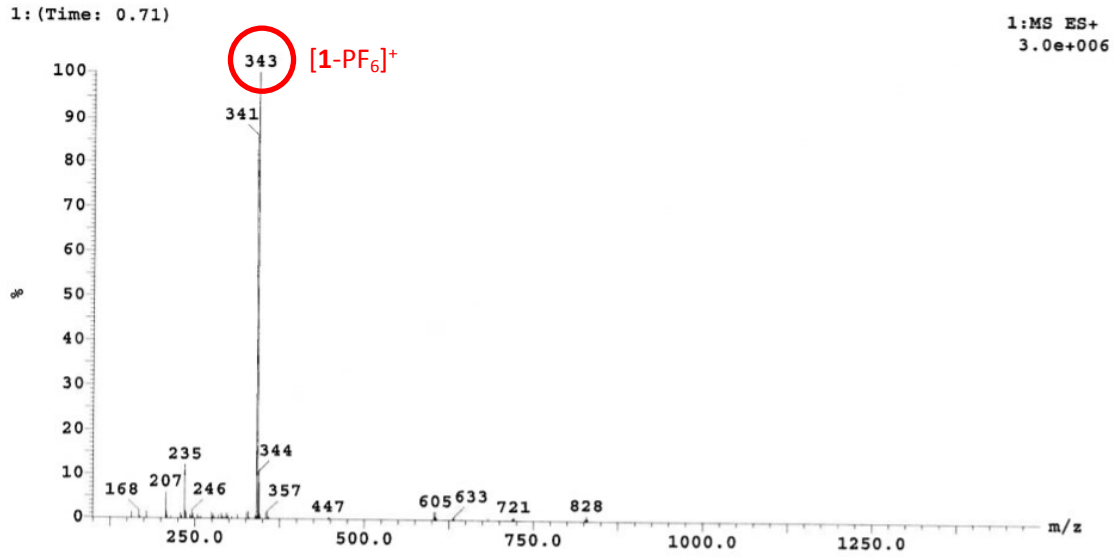

Fig. S12 ESI (positive mode) mass spectrum for compound **1** after 24 h in H_2O:DMSO (100:1) at 37 °C.

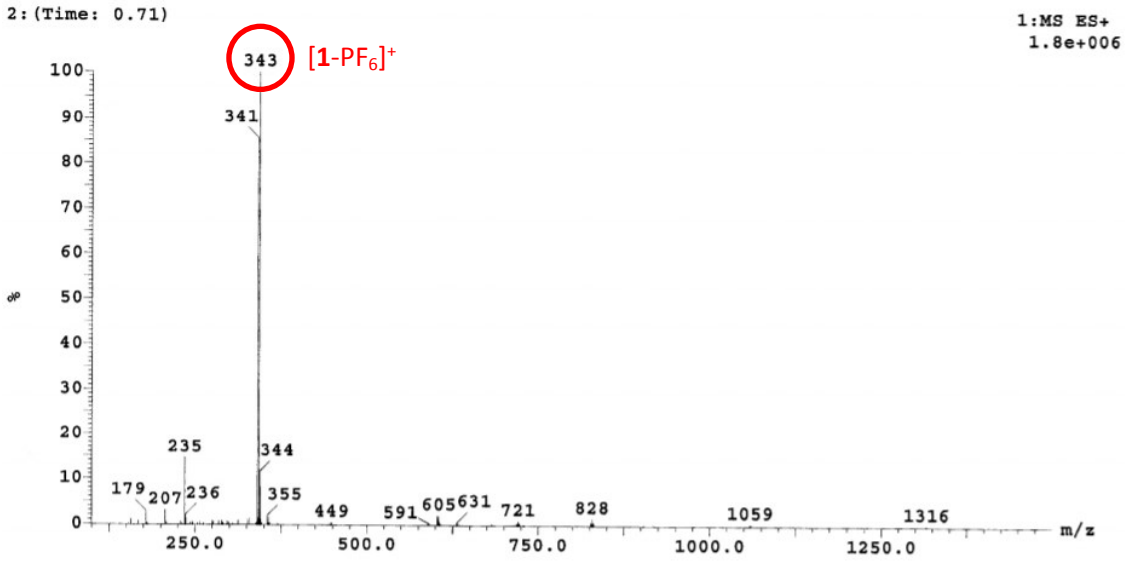

Fig. S13 ESI (positive mode) mass spectrum for compound **1** after 48 h in H_2O:DMSO (100:1) at 37 °C.

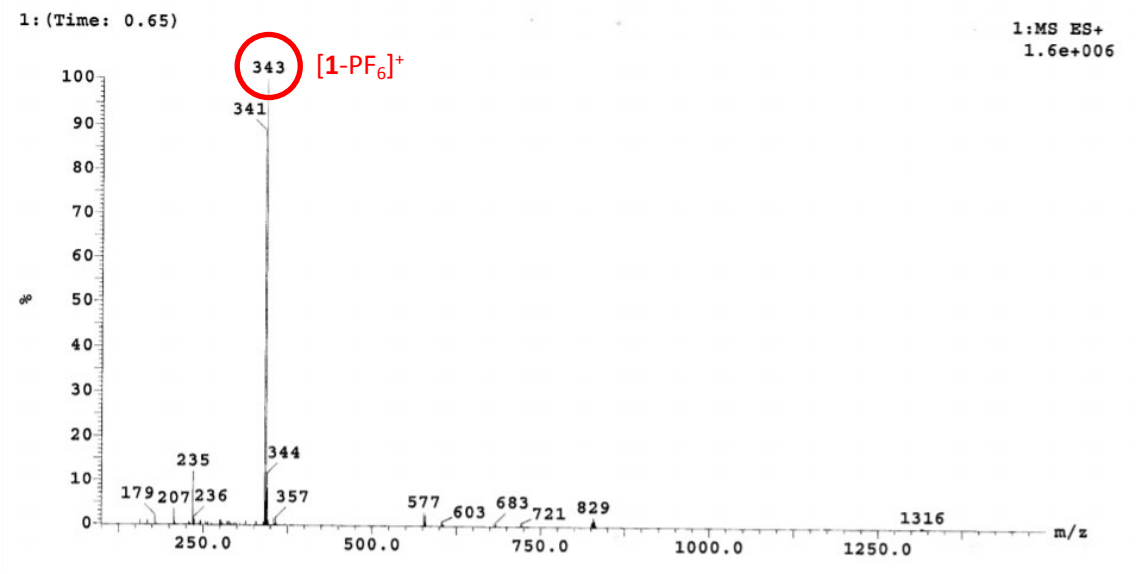

Fig. S14 ESI (positive mode) mass spectrum for compound **1** after 72 h in H_2O:DMSO (100:1) at 37 °C.

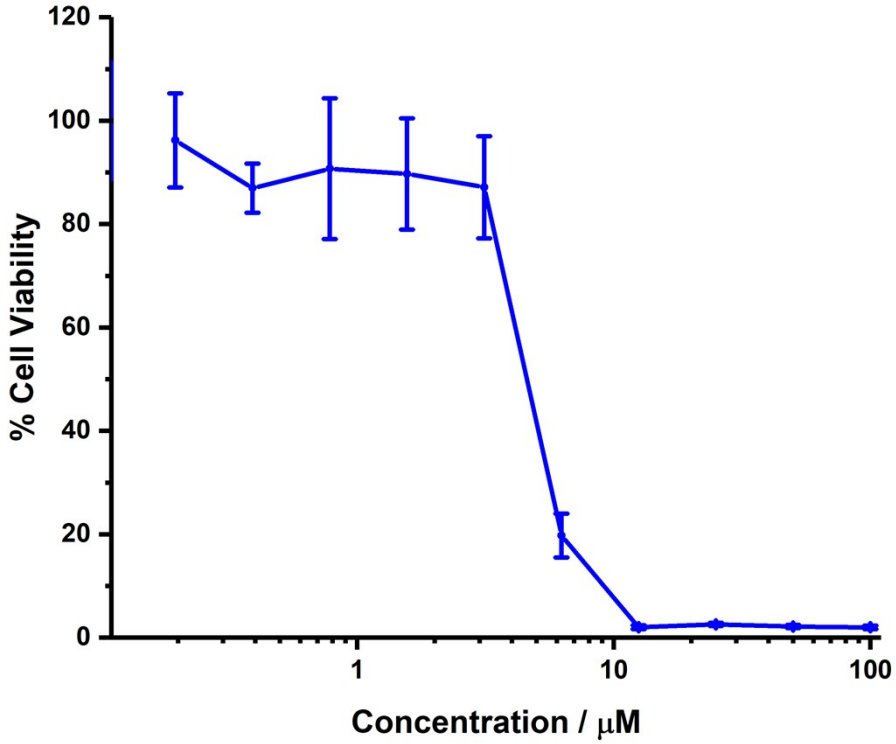

Fig. S15 Cell viability (% of control) vs concentration (μM) for complex **1** in HMLER cells.

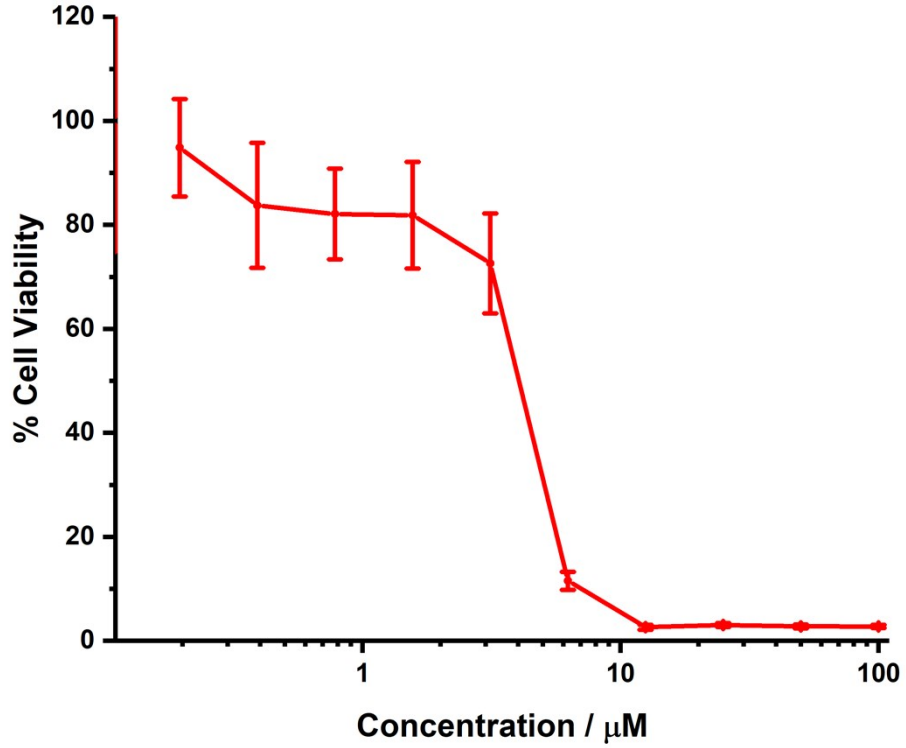

Fig. S16 Cell viability (% of control) vs concentration (μM) for complex **1** in HMLER-shEcad cells.

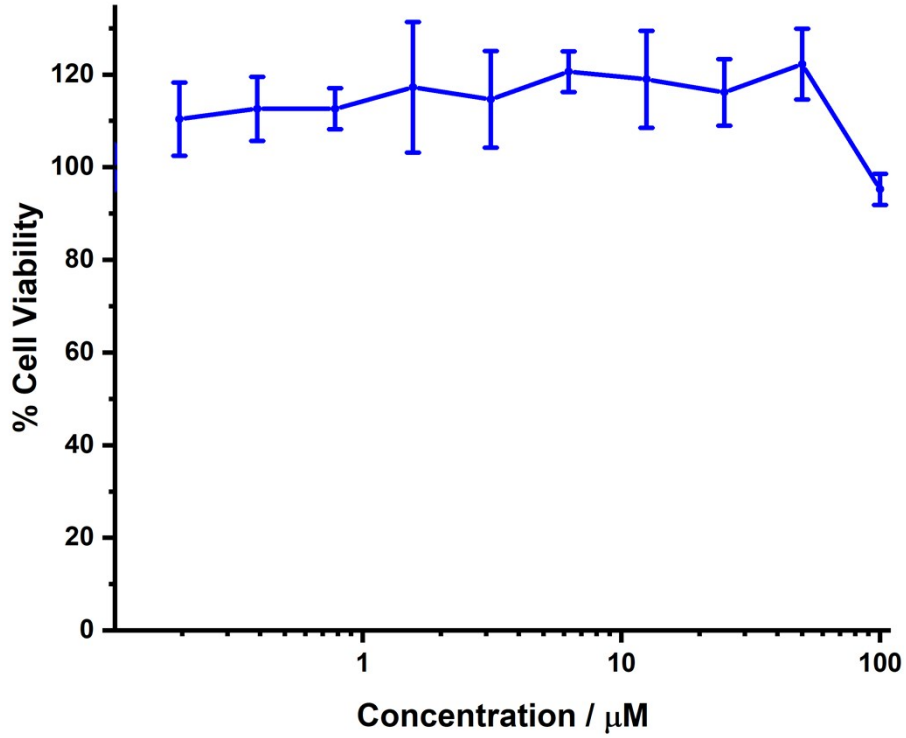

Fig. S17 Cell viability (% of control) vs concentration (μM) for **L**[1] in HMLER cells.

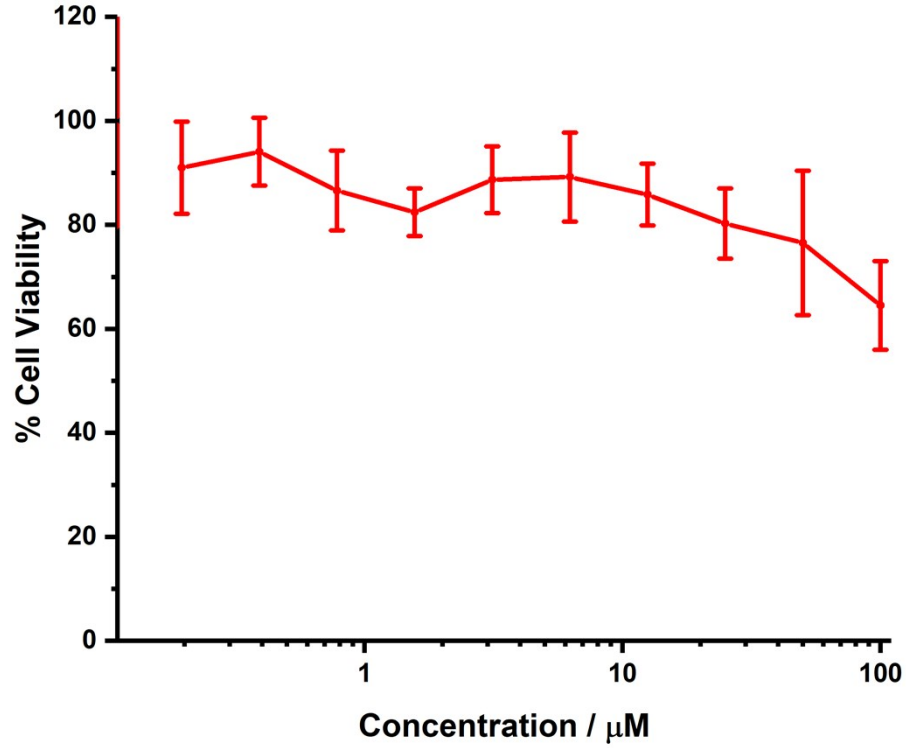

Fig. S18 Cell viability (% of control) vs concentration (μM) for **L**[1] in HMLER-shEcad cells.

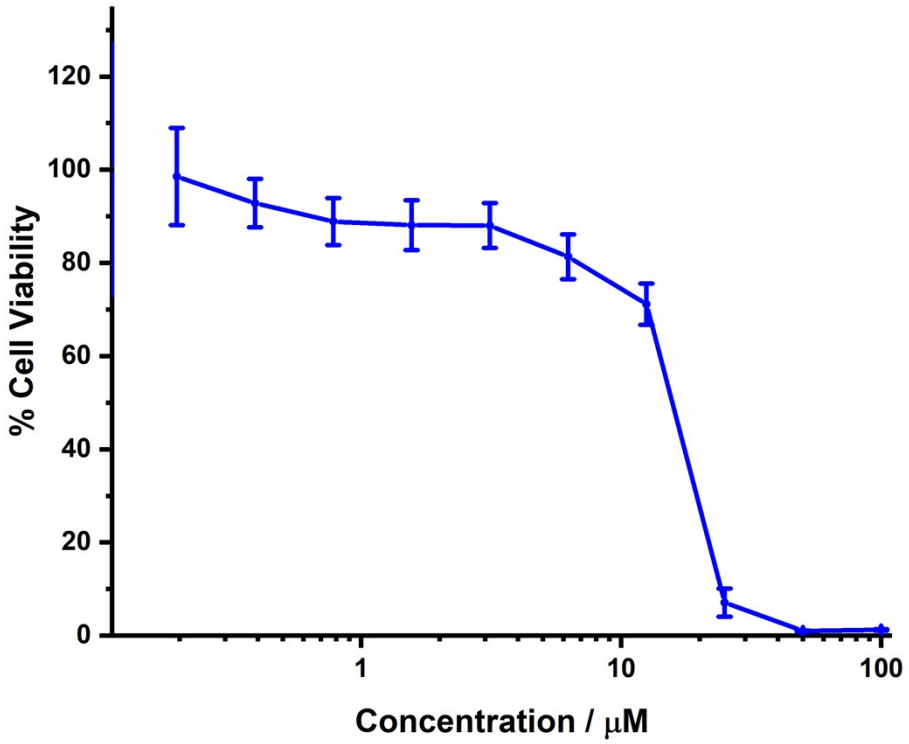

Fig. S19 Cell viability (% of control) vs concentration (μM) for $AgPF_6$ in HMLER cells.

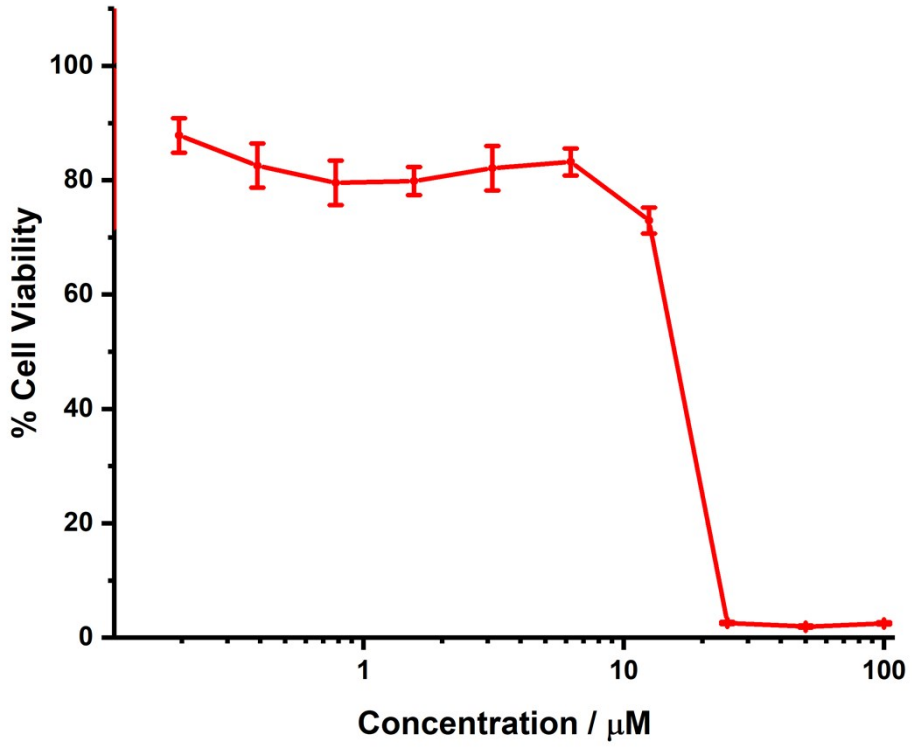

Fig. S20 Cell viability (% of control) vs concentration (μM) for $AgPF_6$ in HMLER-shEcad cells.

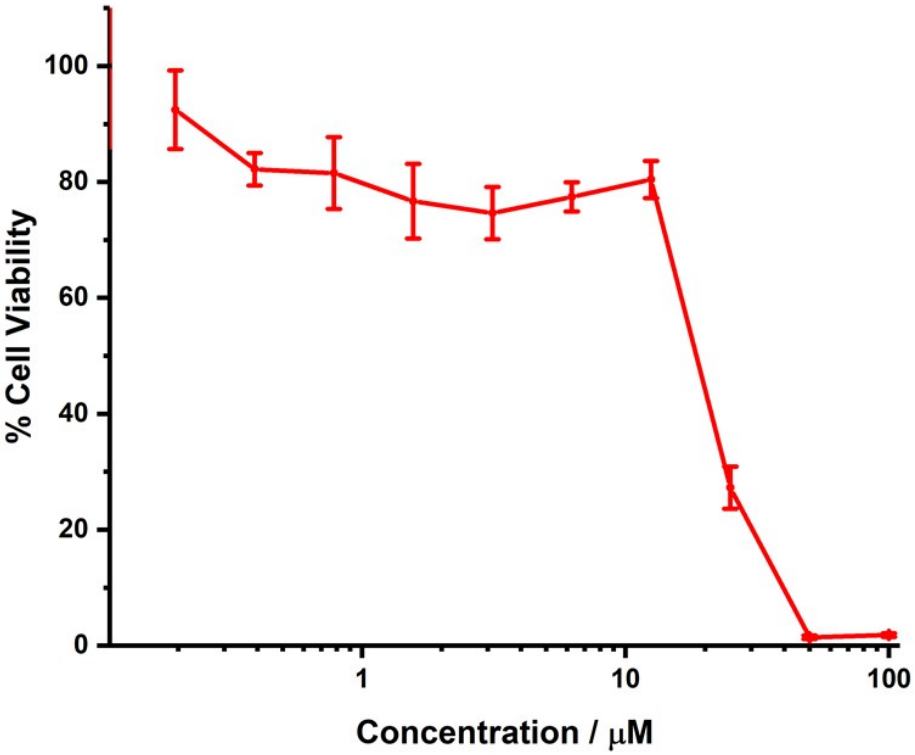

Fig. S21 Cell viability (% of control) vs concentration (μM) for a 1:1 mixture of **L**[1] and $AgPF_6$ in HMLER-shEcad cells.

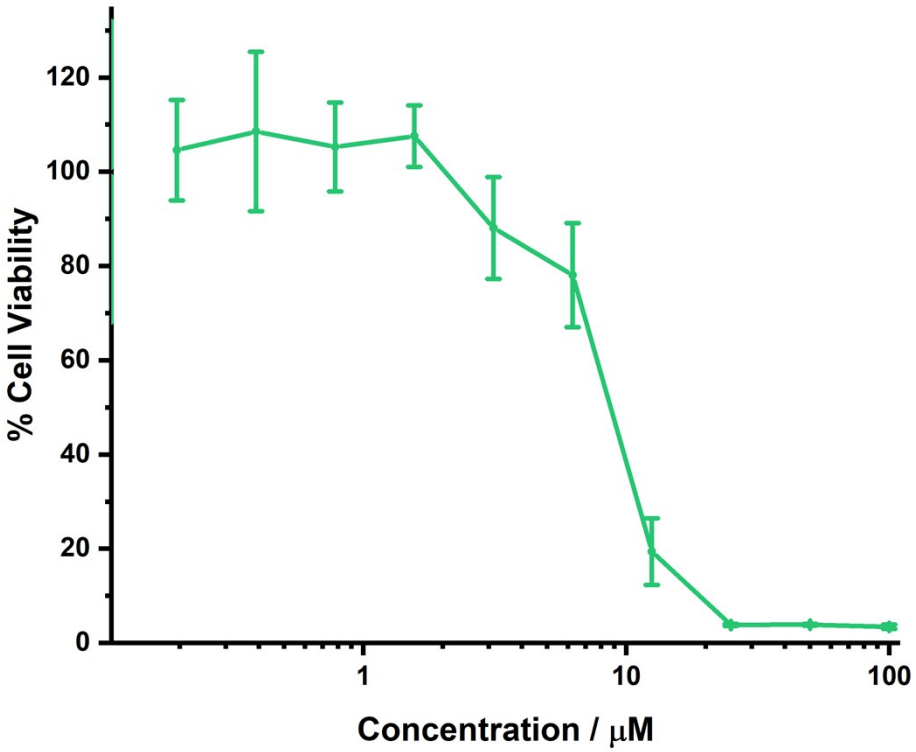

Fig. S22 Cell viability (% of control) vs concentration (μM) for complex **1** in BEAS-2B cells.

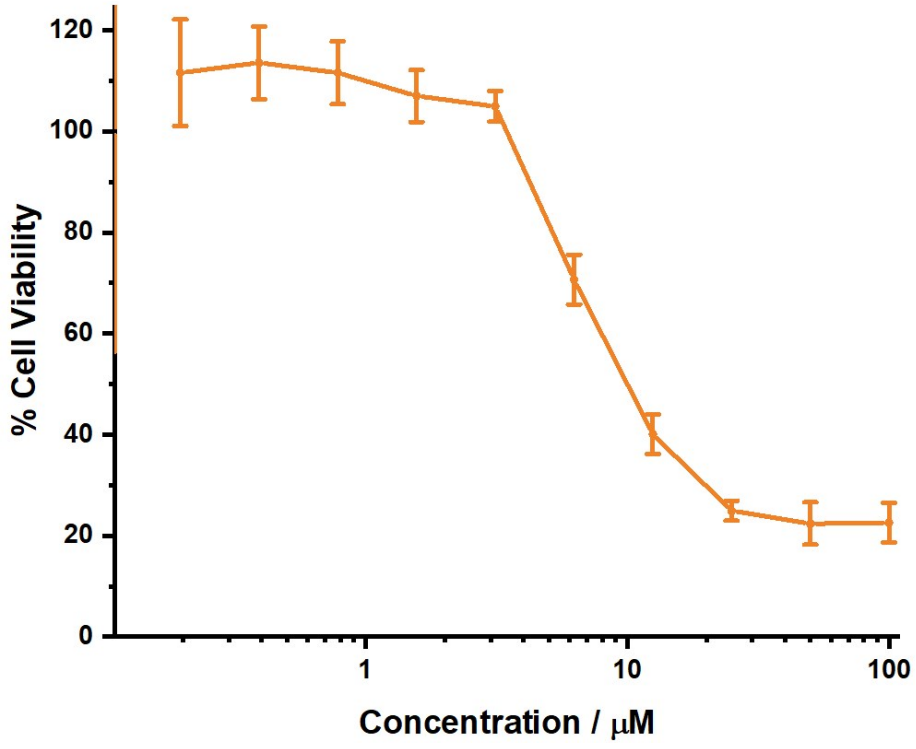

Fig. S23 Cell viability (% of control) vs concentration (μM) for complex **1** in MCF10A cells.

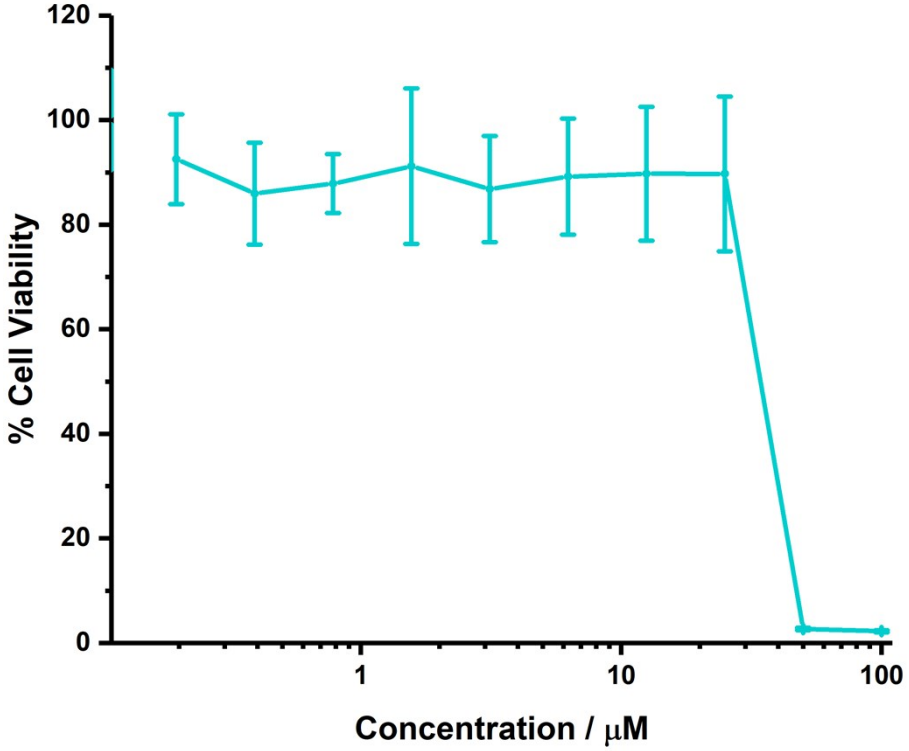

Fig. S24 Cell viability (% of control) vs concentration (μM) for complex **1** in HEK 293 cells.

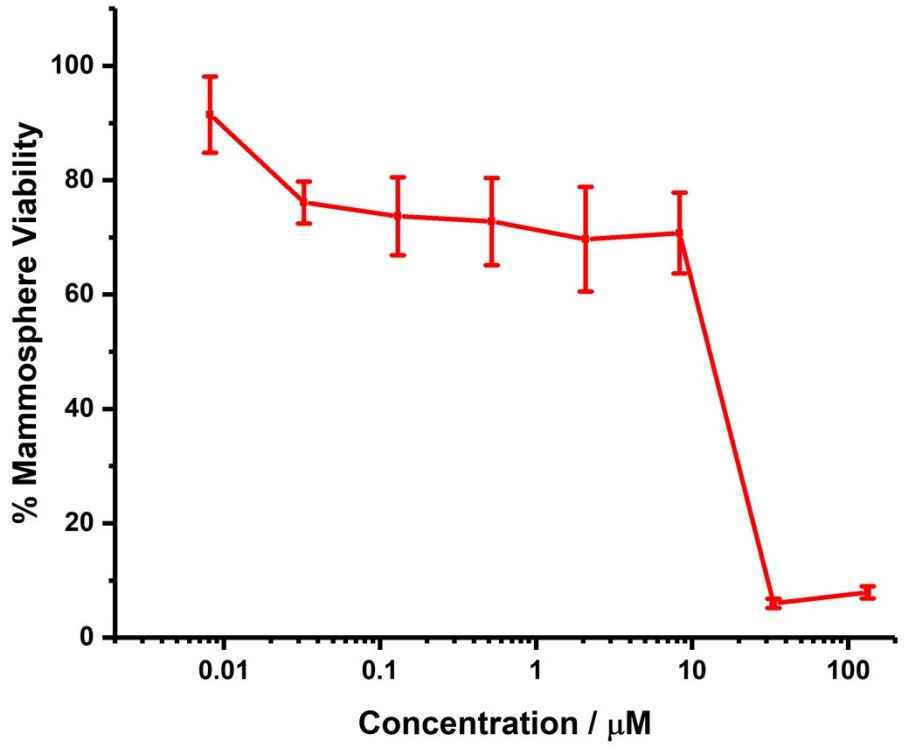

Fig. S25 Mammosphere viability (% of control) vs concentration (μM) for complex **1** in HMLER-shEcad mammospheres.

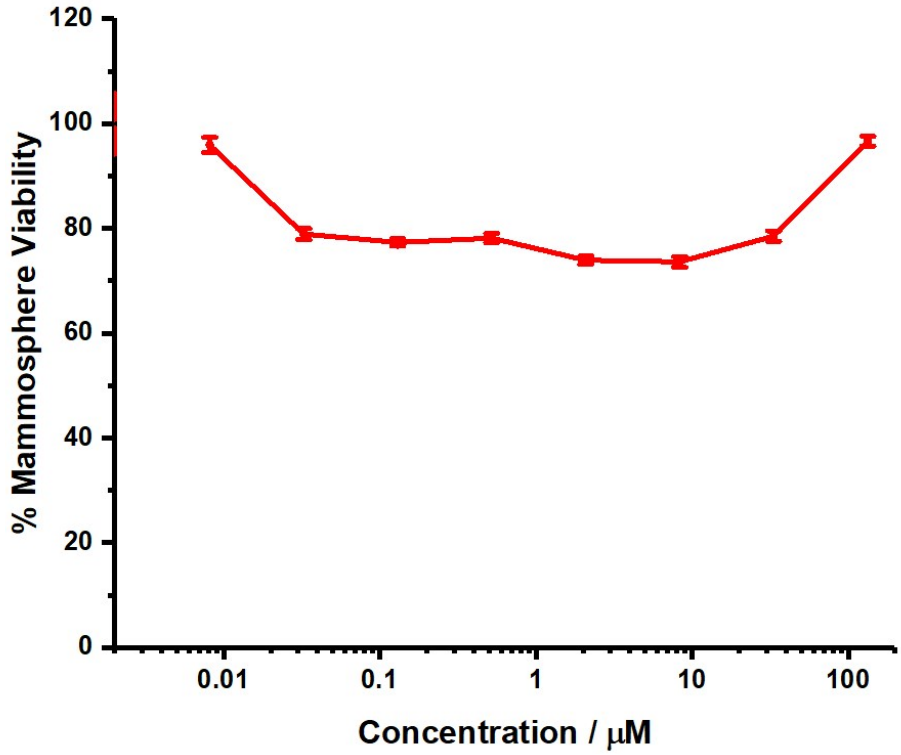

Fig. S26 Mammosphere viability (% of control) vs concentration (μM) for **L**[1] in HMLER-shEcad mammospheres.

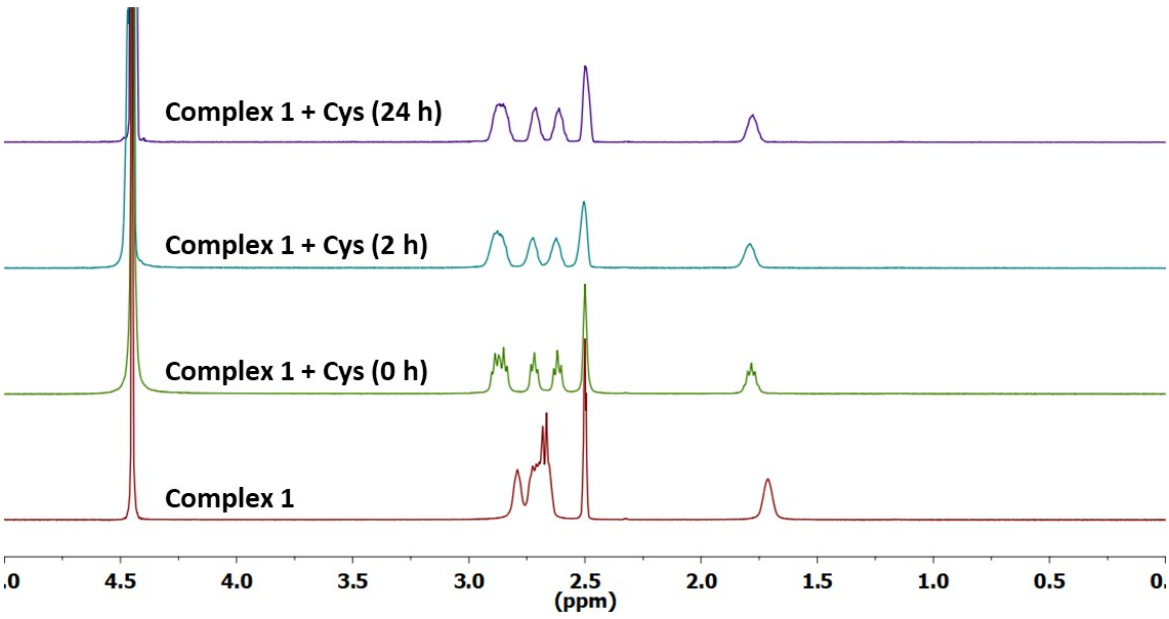

Fig. S27 ^{1}H NMR spectra (400 MHz) for complex **1** (10 mM) in D_2O:DMSO-d_6 (1:1), in the absence and presence of cysteine (Cys, 10 mM) over the course of 24 h at 37 °C.

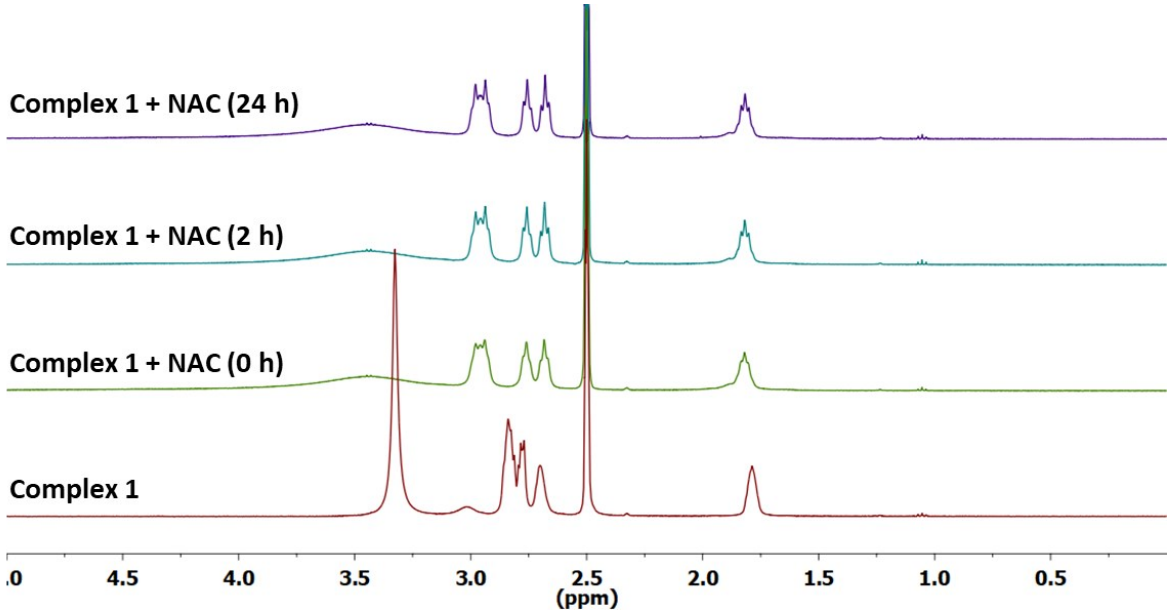

Fig. S28 ^{1}H NMR spectra (400 MHz) for complex **1** (10 mM) in DMSO-d_6, in the absence and presence of *N*-acetylcysteine (NAC, 10 mM) over the course of 24 h at 37 °C.

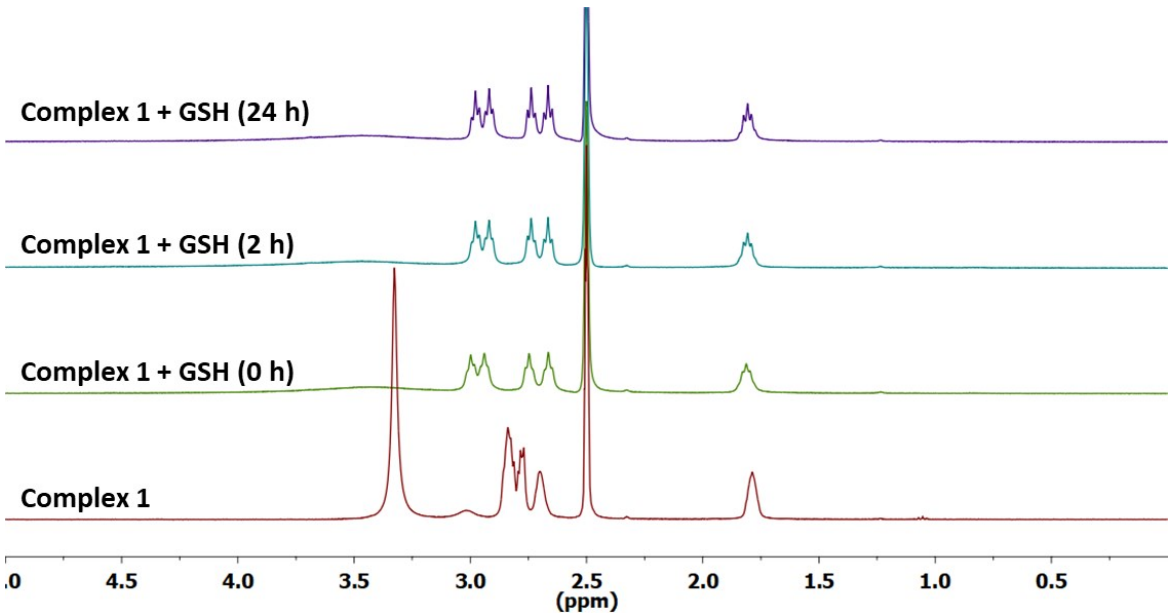

Fig. S29 ^{1}H NMR spectra (400 MHz) for complex **1** (10 mM) in DMSO-d_6, in the absence and presence of glutathione (GSH, 10 mM) over the course of 24 h at 37 °C.

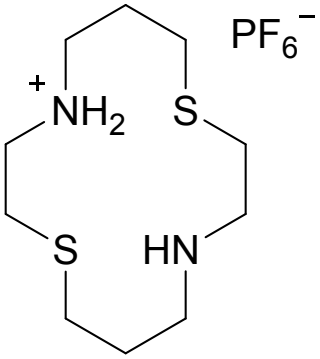

L¹-H⁺

Fig. S30 Chemical structure of the mono-protonated analogue of **L¹**, **L¹-H⁺**.

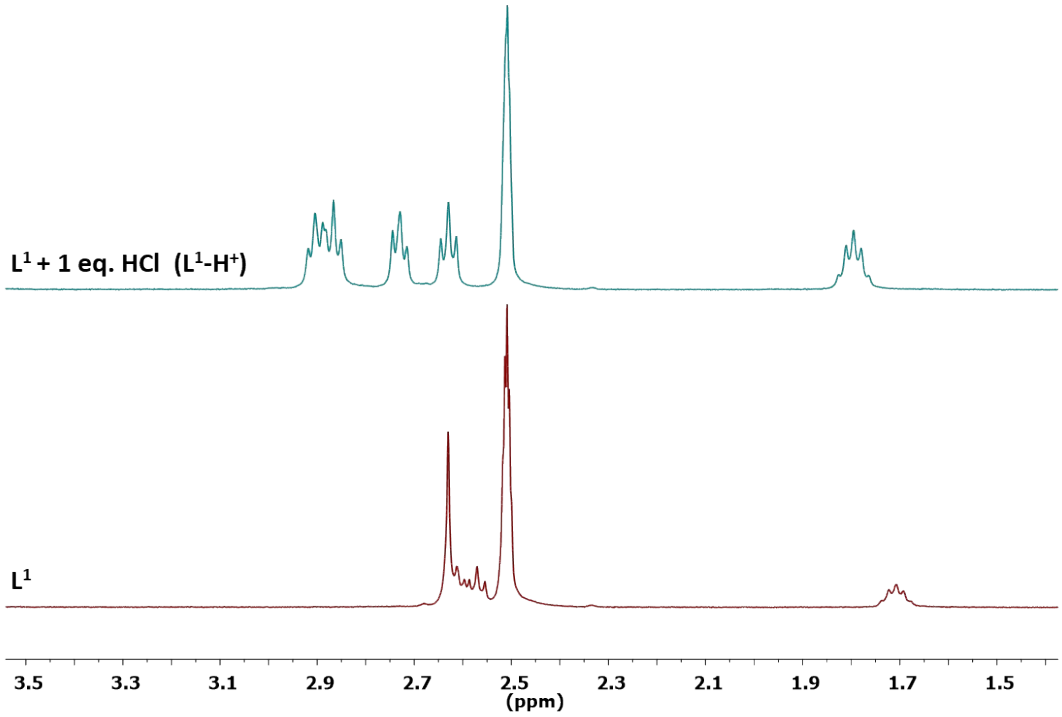

Fig. S31 ^{1}H NMR spectra (400 MHz) for **L¹** (10 mM) in D_2O:DMSO-d_6 (1:1), in the absence and presence of HCl (10 mM) after 30 min incubation at 37 °C. The latter represents the ^{1}H NMR spectrum (400 MHz) for the mono-protonated analogue of **L¹**, **L¹-H⁺** in D_2O:DMSO-d_6 (1:1).

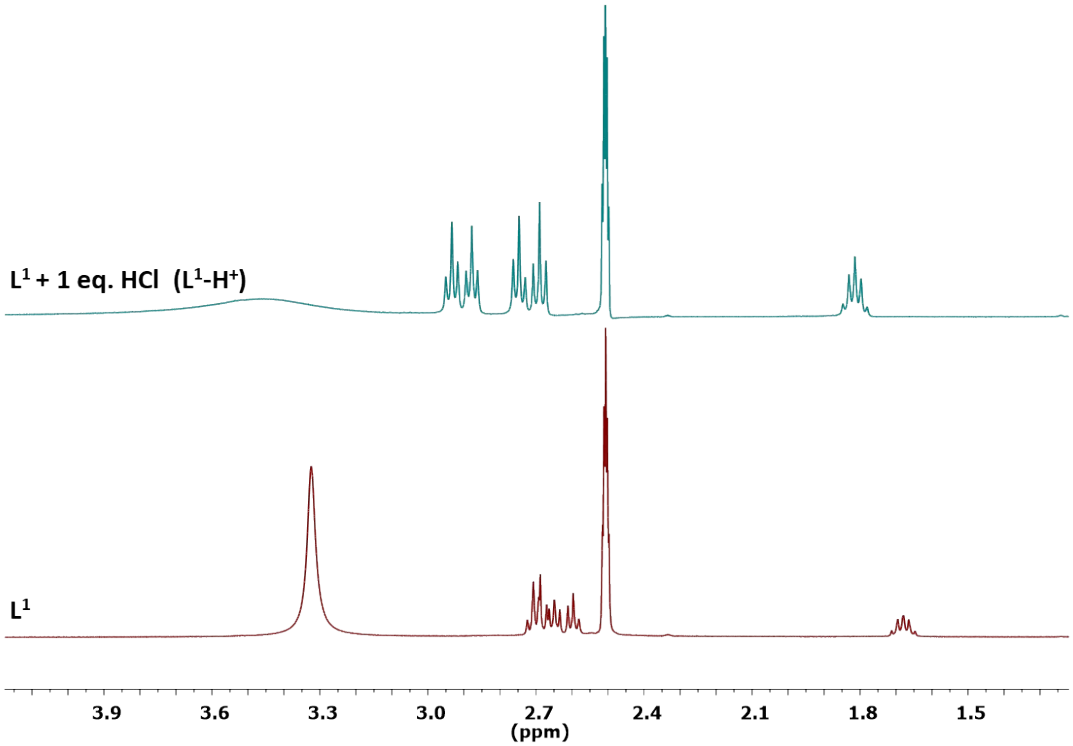

Fig. S32 ^{1}H NMR spectra (400 MHz) for **L^{1}** (10 mM) in DMSO-d_6, in the absence and presence of HCl (10 mM) after 30 min incubation at 37 °C. The latter represents the ^{1}H NMR spectrum (400 MHz) for the mono-protonated analogue of **L^{1}**, **L^{1}-H^{+}** in DMSO-d_6.

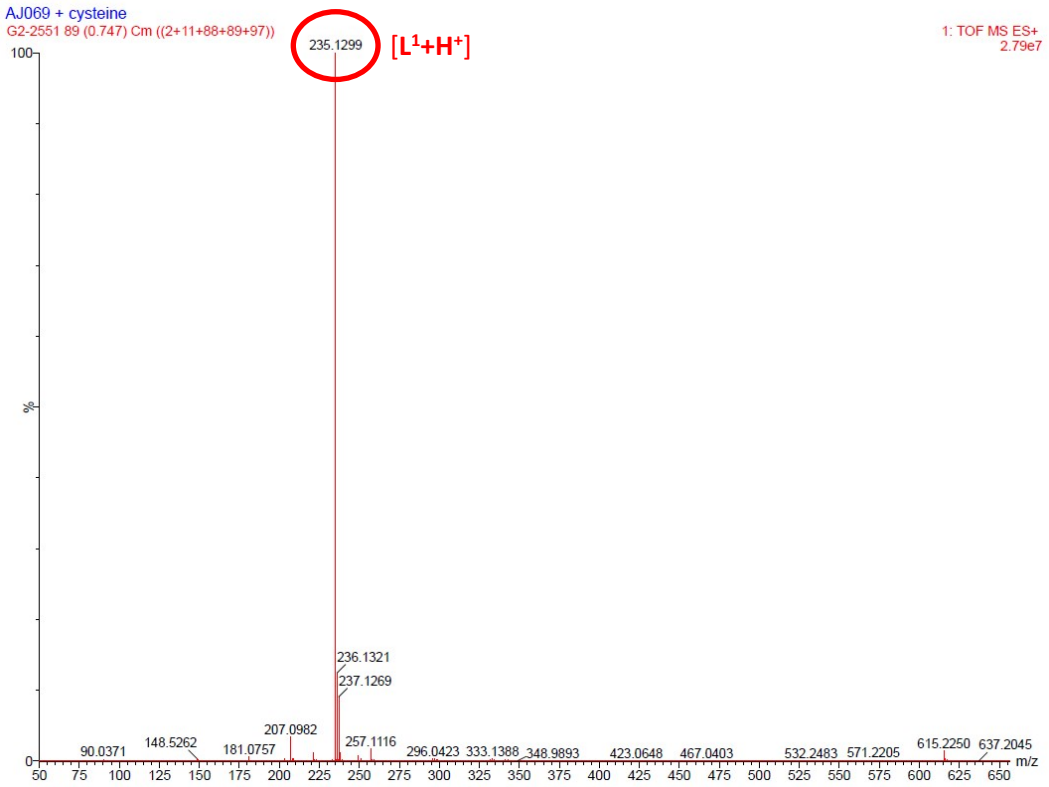

Fig. S33 High-resolution ESI-QTOF mass spectrum for the reaction solution of complex **1** (10 mM) with cysteine (Cys, 10 mM) in H_2O:DMSO (1:1) after 24 h incubation at 37 °C.

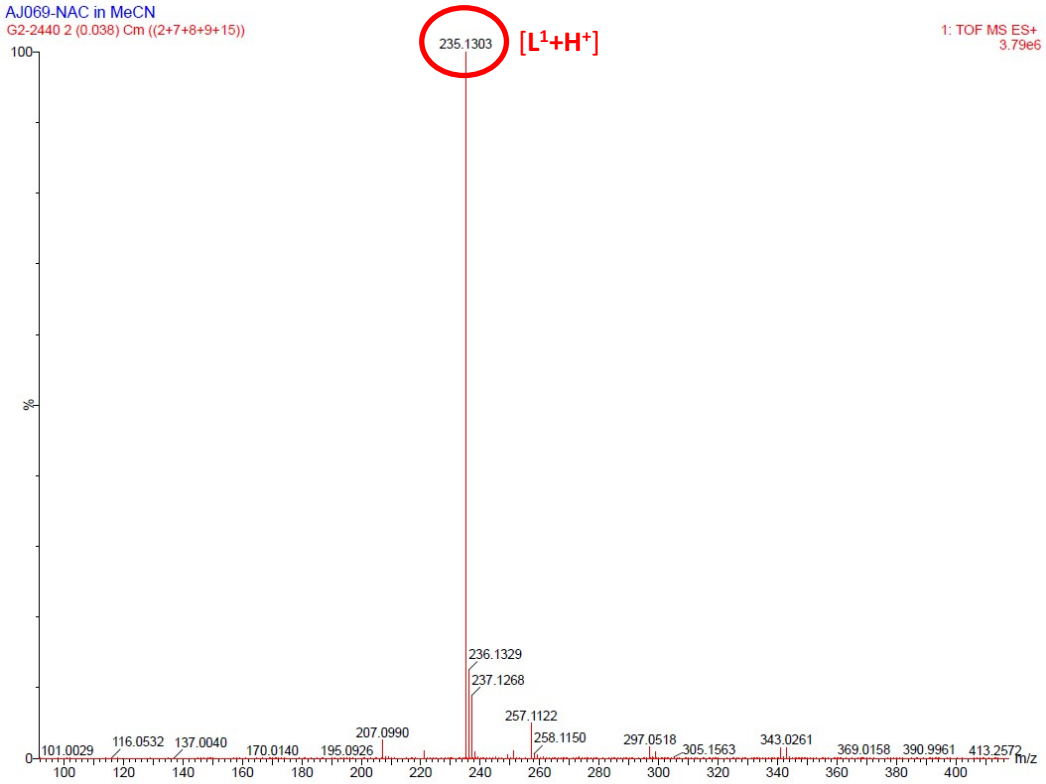

Fig. S34 High-resolution ESI-QTOF mass spectrum for the reaction solution of complex **1** (10 mM) with *N*-acetylcysteine (NAC, 10 mM) in DMSO after 24 h incubation at 37 °C.

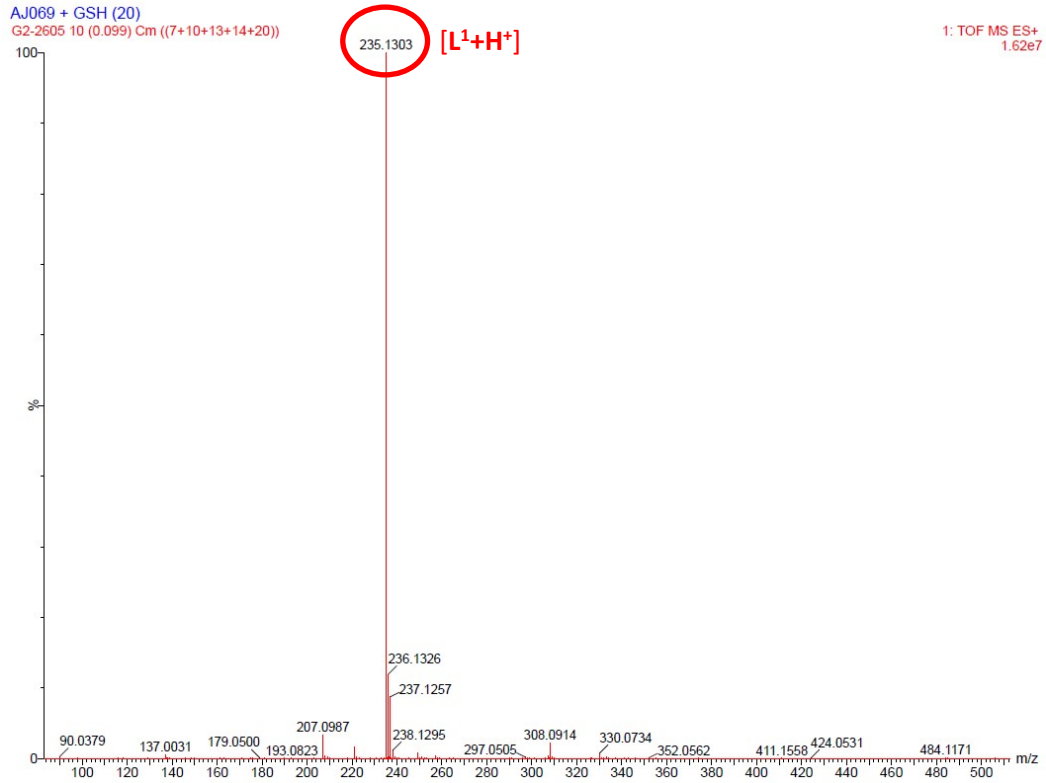

Fig. S35 High-resolution ESI-QTOF mass spectrum for the reaction solution of complex **1** (10 mM) with glutathione (GSH, 10 mM) in DMSO after 24 h incubation at 37 °C.

Table S3. ICP-MS data displaying the proportion of silver present in the reaction solution and precipitate upon reaction of complex **1** (10 mM) with cysteine (Cys, 10 mM) in H_2O:DMSO (1:1) after 24 h at 37 °C.

	Solution	Precipitate
^{107}Ag (STD) / ppb	4.79	125272.64
^{107}Ag (KED) / ppb	4.82	127313.84
^{109}Ag (STD) / ppb	4.84	128676.16
^{109}Ag (KED) / ppb	4.78	125981.82
Ag Avg / ppb	4.81	126811.11
Error (SD) / ppb	0.02	1302.47
Volume / ml	4.25	4.25
Mass Ag / µg	0.02	538.95
Error	9.67×10^{-6}	5.54
% of initial Ag	**0.0038**	**99.93**

Table S4. ICP-MS data displaying the proportion of silver present in the reaction solution and precipitate upon reaction of complex **1** (10 mM) with *N*-acetylcysteine (NAC, 10 mM) in DMSO after 24 h at 37 °C.

	Solution	Precipitate
^{107}Ag (STD) / ppb	10711.50	84418.14
^{107}Ag (KED) / ppb	10727.84	85637.56
^{109}Ag (STD) / ppb	10754.53	83892.49
^{109}Ag (KED) / ppb	10754.53	85766.28
Ag Avg / ppb	10737.10	84928.62
Error (SD) / ppb	18.36	398.31
Volume / ml	4.25	4.25
Mass Ag / µg	45.6	364.51
Error	0.08	1.69
% of initial Ag	**16.92**	**67.58**

Table S5. ICP-MS data displaying the proportion of silver present in the reaction solution and precipitate upon reaction of complex **1** (10 mM) with glutathione (GSH, 10 mM) in DMSO after 24 h at 37 °C.

	Solution	Precipitate
^{107}Ag (STD) / ppb	< limit of detection	113217.7
^{107}Ag (KED) / ppb	< limit of detection	114150.9
^{109}Ag (STD) / ppb	< limit of detection	113078.8
^{109}Ag (KED) / ppb	< limit of detection	116750.5
Ag Avg / ppb	0	114299.5
Error (SD) / ppb	N/A	1701.93
Volume / ml	4.25	4.25
Mass Ag / µg	0	485.77
Error	N/A	7.23
% of initial Ag	**0**	**90.1**

Scheme S1. Representative scheme for the reaction of **1** with biologically relevant thiol-containing compounds such as cysteine, *N*-acetylcysteine, or glutathione.

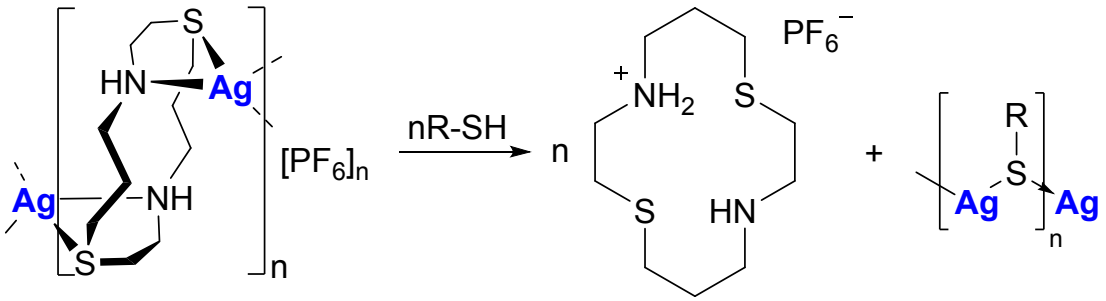

1 **L^1-H^+**

(R-SH = cysteine, *N*-acetylcysteine, or glutathione)

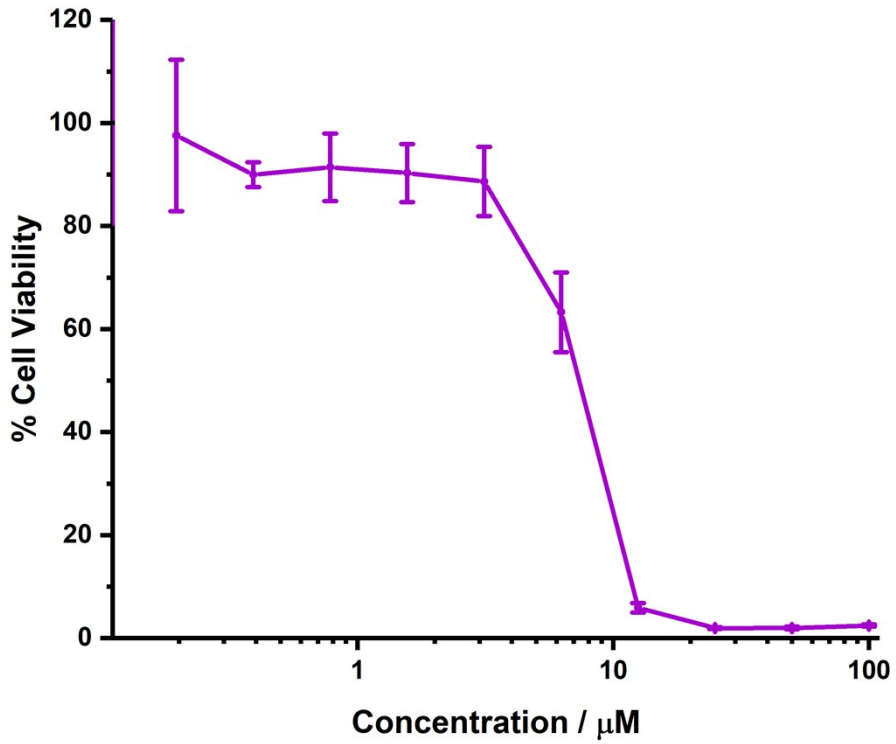

Fig. S36 Cell viability (% of control) vs concentration (μM) for complex **1** in HMLER-shEcad cells in the presence of z-VAD-FMK (5 μM).

References

1. P. Gerschel, K. Warm, E. R. Farquhar, U. Englert, M. L. Reback, D. Siegmund, K. Ray and U. P. Apfel, *Dalton Trans.*, 2019, **48**, 5923-5932.
2. G. Sheldrick, *University of Göttingen, Germany*, 1996.
3. *CrysAlisPro, Agilent Technologies, Version 1.171.35.11. Multi-scans absorption correction with SCALE3 ABSPACK scaling algorithm.*
4. G. M. Sheldrick, *Acta Crystallogr. Sect. C*, 2015, **71**, 3-8.